ELSEVIER

Chemical Engineering Journal 81 (2001) 281–285

Chemical Engineering Journal

www.elsevier.com/locate/cej

Permeation of gases in industrial porous catalysts

Pavel Čapek [a,*], Vladimír Hejtmánek [b], Olga Šolcová [b]

[a] *Department of Organic Technology, Prague Institute of Chemical Technology, Technická 5, 16628 Prague 6, Czech Republic*
[b] *Institute of Chemical Process Fundamentals, Academy of Sciences of the Czech Republic, Rozvojová 135, 16502 Prague 6, Czech Republic*

Received 15 November 1999; received in revised form 3 April 2000; accepted 16 May 2000

Abstract

An experimental method for determination of porous solid texture was proposed and verified. The method is based on unsteady permeation of single gases in a porous medium. Transport parameters characterizing porous materials were determined by fitting the experimental data to the theoretical transient responses by minimizing the objective function. Confidence limits of the transport parameters were evaluated on the base of the Beale criterion. Results were discussed in terms of different mechanisms of mass transport. Advantages of this technique were demonstrated for three porous catalysts of different textures.

Keywords: Permeation of gases; Porous materials; Transport parameters of porous solids

1. Introduction

Porous materials play an important role in many chemical processes such as heterogeneously catalyzed reactions, adsorption, and gas–solid reactions. If mass transport is not much faster than other physical and chemical phenomena, significant gradients of composition and/or pressure may appear within the porous structure. The diffusional and/or permeation flux arisen inside pores as consequence of these gradients has not a negligible influence on the reaction kinetics, the adsorption equilibrium, the vapor–liquid equilibrium, etc. For evaluation of a real pore network, mercury porosimetry in combination with low-temperature physical adsorption of inert gases is commonly used. However, these methods do not provide information suitable for calculation of concentration fields inside porous solid particles under different conditions (temperature, pressure, and composition of multicomponent mixtures). For this reason, several experimental techniques and theories for direct characterization of mass transport in porous solids have been proposed and validated. Experiments are usually performed in the Wick–Kallenbach cell [1] or in its modified version [2–4]. A particularly useful theory is based on the Maxwell–Stefan equations modified for mass transport in porous solids [5–7]. This theory distinguishes between transport properties of gases and textural properties of porous solids characterized by the set of transport parameters of porous solids. Transport properties of gases are usually known. However, transport parameters are not accessible on a theoretical basis and have to be determined experimentally. The simplest experimental technique uses the forced flow of a single gas through a porous solid (permeation). This method allows to assess a porous solid texture and to estimate some of transport parameters needed for description of multicomponent mass transport [3].

The transport of a single gas in a long cylindrical pore can be characterized by the magnitude of the Knudsen number. For this purpose, the Knudsen number is defined as the ratio of the mean free path of the molecule λ to the mean pore diameter $2\langle r\rangle$

$$Kn = \frac{\lambda}{2\langle r\rangle} \tag{1}$$

In the Knudsen region, i.e. if pressure $\to 0$ and hence $Kn \to \infty$, the encounters of molecules with pore walls prevail. On the other hand, in the region of continuum, i.e. if pressure is sufficiently high and hence $Kn \to 0$, the most of encounters takes place among molecules. Both the mechanisms contribute to the overall mass transport in the transition region ($Kn \approx 1$).

The relation expressing the molar flux density of a single gas both in the Knudsen flow and the viscous flow with the slip on the wall is given by the d'Arcy constitutive equation

$$N = -B\frac{\partial c}{\partial x} \tag{2}$$

* Corresponding author.
E-mail address: hejtmanek@icpf.cas.cz (V. Hejtmánek).

1385-8947/01/$ – see front matter
PII: S1385-8947(00)00192-3

where c is the molar concentration, x the spatial coordinate and B denotes an effective permeability coefficient generally depending on pressure P and temperature T and porous solid properties. For this dependence, the Weber equation is often used

$$B = \frac{2}{3}\langle r\rangle\psi\sqrt{\frac{8R_gT}{\pi M}}\left(\frac{\omega + Kn}{1 + Kn}\right) + \langle r^2\rangle\psi\frac{P}{8\mu} \quad (3)$$

where $\langle r^2\rangle$ designates the mean square of pore radii, R_g denotes the gas constant, M the molecular weight of gas, and μ the gas viscosity. The mean pore radius and the mean square of pore radii appear always in the product with the ratio ψ of the total porosity ε and tortuosity. The parameter ω characterizes the slip of molecules on the pore wall. According to the Weber equation there are the four material constants of a porous solid: $\langle r\rangle\psi$, $\langle r^2\rangle\psi$, $\langle r\rangle$ and ω. For the sake of simplicity, the parameter ω was supposed to be 1 and, thus, the Weber equation (3) could be simplified in the following manner:

$$B = \frac{2}{3}\langle r\rangle\psi\sqrt{\frac{8R_gT}{\pi M}} + \langle r^2\rangle\psi\frac{P}{8\mu} \quad (4)$$

For any inert gas and a porous solid, given the viscosity μ and the molecular weight M shall balance differences in the corresponding actual molar flux density (Eq. (2)) in order that the transport parameters $\langle r\rangle$ and $\langle r^2\rangle\psi$ may be constant.

The main goal of this study has been the proposal and the validation of an experimental method for determination of the transport parameters $\langle r\rangle$ and $\langle r^2\rangle\psi$ from measurements performed under dynamic conditions in the permeation cell. Parameter estimates have been supplemented by their confidence limits in order to judge the experimental technique performance. Three catalysts of different textures have been used to demonstrate the features of our method.

2. Experimental

Three porous catalysts of different textures were selected for the purpose of this study. The first two catalysts are used in the chemical industry for methanol synthesis (ICI 52-1, ICI Ltd., UK) and hydrogenation (Cherox 42-00, Chemopetrol Litvínov, Inc., Czech Republic, the shorter name Cherox is used in the foregoing discussion). The third catalyst was α-alumina (internally marked by A5) prepared from boehmit Pural SB, Condea Chemie, Germany. All porous materials were shaped as cylindrical pellets. Their basic textural properties were obtained by the standard methods of textural analysis, see Table 1. The catalysts ICI 52-1 and Cherox 42-00 were both monodispersed differing in the mean pore radii. Pellets of A5 had the bidispersed texture in which mesopores dominated over macropores.

The permeation cell (Fig. 1) consisted of two chambers separated by a metallic holder of pellets. Cylindrical porous pellets were sealed by pieces of a silicon rubber in the holder. The capillary of the small internal diameter connected the upper chamber and the electromagnetic valve. It was checked that its diameter of 0.98 mm and its length of 15 cm were sufficient to guarantee the smooth filling of the upper chamber. The lower chamber was equipped by the absolute pressure gauge (0–101 kPa, Omega Engineering, Inc., USA). The valve opening and signal recording were synchronized by means of a personal computer.

Table 1
Basic textural parameters of porous materials

Quantity	ICI 52-1	Cherox	A5
Pellet height, L (mm)	4.27	4.90	3.45
Pellet diameter (mm)	4.86	5.00	3.45
Volume[a], V_p (cm^3)	3.327	4.041	0.032
Helium density ($g\,cm^{-3}$)	3.833	3.472	3.953
Apparent density ($g\,cm^{-3}$)	1.518	2.234	2.548
Total porosity, ε	0.604	0.357	0.355
Surface BET ($m^2\,g^{-1}$)	73.0	3.97	0.46
Mean pore radius[b] (nm)	8.2	70	290/2070

[a] Total volume of all pellets inserted in the pellet holder.
[b] Determined by mercury porosimetry.

All permeation experiments were made under an ambient temperature. The number of pellets, i.e. the total pellet area for mass transport and, consequently, a time span of experiment, was adjusted according to pellet properties (see Table 1). Before the start of the run, the same values of pressure were adjusted in both the chambers. At the start of the run, the electromagnetic valve was opened and the selected inert gas flowing through the input capillary started to fill the upper chamber. From this moment (t=0 s) the pressure response in the lower chamber was logged by the personal computer with frequency of 1 Hz. The pressure in the upper chamber and the pressure in front of the input capillary were equilibrated within a few seconds. Thus, the duration of this process was negligible in comparison with the duration of the whole experiment (>300 s). Inert gases — H_2, He, N_2, and Ar — were used in all experiments.

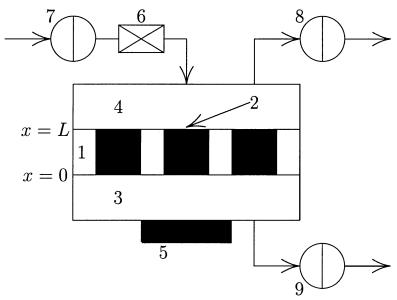

Fig. 1. Scheme of the permeation cell. 1, Metallic holder of pellets; 2, pellets; 3, lower chamber of volume V_0=73.6 cm^3; 4, upper chamber of volume V_L=78.5 cm^3; 5, pressure gauge; 6, capillary; 7, input valve; 8 and 9, vacuum valves.

3. Mass balance of the permeation cell

Since the metallic pellet holder closes pellet shells, mass transport in porous pellets can be treated as one-dimensional, i.e. the porous pellet body has the slab geometry. Thus, the mass balance of gaseous phase in porous pellets reads

$$\varepsilon \frac{\partial c(t,x)}{\partial t} = -\frac{\partial N(t,x)}{\partial x} \tag{5}$$

where c is the molar concentration generally dependent on the spatial coordinate x and time t. The molar flux density N is given by Eq. (2).

The boundary condition at $x=0$ is given by the mass balance of the lower chamber. Assuming a gradientless chamber, this condition reads

$$V_0 \frac{\partial c(t,0)}{\partial t} = -\frac{V_\mathrm{p}}{L} N(t,0) \tag{6}$$

where V_0 is the volume of the lower chamber, V_p denotes the total volume of all pellets and L is the mean pellet length (height in Table 1). The boundary condition at $x=L$ is given by mass balance of the upper chamber of the volume V_L

$$V_L \frac{\partial C(t,L)}{\partial t} = \frac{V_\mathrm{p}}{L} N(t,L) + \frac{\pi \xi}{16 R_\mathrm{g} T \mu} \{P_\mathrm{in}^2 - [R_\mathrm{g} T c(t,L)]^2\} \tag{7}$$

No pressure gradient in the chamber was again assumed in derivation of Eq. (7). The last term on the right-hand side of Eq. (7) — the Hagen–Poiseuille law — describes the forced flow through the input capillary. The input pressure in front of the capillary P_in is the constant quantity as well as the gas viscosity μ. The constant ξ determines a capillary resistance to the viscous flow.

Initial conditions for differential equations (2) and (4)–(7) are given by the following expression:

$$c(0,x) = c^0 \tag{8}$$

where the molar concentration c^0 is proportional to the initial pressure in the cell. The initial boundary value problems (2) and (4)–(8) was integrated by the method of lines [8].

4. Results and discussion

The adjustable constant ξ in Eq. (7) was calculated from the capillary diameter and length, i.e. $\xi = 3.9\times10^{-13}\,\mathrm{m}^3$. Preliminary numerical simulations revealed that the model was capable of predicting a reliable pressure rise in the upper chamber after the start of the run despite of the turbulent flow in the input capillary. Hence, it appears that the approximate validity of the second term in the right-hand side of Eq. (7) did not affect the performance of the complete models (2) and (4)–(8). Five pressure responses differing in initial pressure levels were obtained for each single gas. To estimate a performance of our method, each measurement was repeated once. The initial molar concentration c^0 in Eq. (8) was determined from the experimental value of the initial pressure in the cell for each run. The standard deviation σ of measured pressure p_{ij} was approximately 0.35 kPa in the whole working interval of the pressure gauge.

The transport parameters should only depend on the porous solid used. However, random errors of measured quantities result generally in disapproving values of parameters estimated from different experiments and, thus, an appropriate way of their averaging must be chosen. In this work, the transport parameters were obtained by fitting the experimental data for all the gases and the given porous catalyst to the systems (2) and (4)–(8) by minimizing the weighted sum of squared deviations between the experimental (p_{ij}) and theoretical ($\sim c(t_{ij},0)$) pressure responses

$$\chi^2(\langle r\rangle\psi, \langle r^2\rangle\psi) = \frac{1}{\sigma^2}\sum_{j=1}^{m}\frac{1}{n_j}\sum_{i=1}^{n_j}[p_{ij} - R_\mathrm{g} T c(t_{ij},0)]^2 \tag{9}$$

Since combinations of the five initial pressure levels (see Fig. 2) and the four gases (H_2, He, N_2, and Ar) were used once, the total number of responses m was always 20. The minimization of the objective function (9) was performed by the Marquardt–Levenberg method [8,9] which required the vector of partial derivatives

$$\Omega(t) = \{\omega_1(t), \omega_2(t)\} = \left\{ R_\mathrm{g} T \frac{\partial c(t,0)}{\partial \ln(\langle r\rangle\psi)}, R_\mathrm{g} T \frac{\partial c(t,0)}{\partial \ln(\langle r^2\rangle\psi)} \right\} \tag{10}$$

To get these derivatives, equations for sensitivity functions [10] were solved together with the system of Eqs. (2) and (4)–(8). The Marquardt–Levenberg method always converged within several iterations in all cases.

Fig. 2 depicts a very good agreement between experimental and theoretical responses for permeation of He and N_2 through pellets of Cherox. A similarly good agreement was found for ICI 52-1 and A5. The optimum transport parameter values are listed in Table 2. The model fits the experimental data in the descending order: ICI 52-1, Cherox, and A5. A relatively poor fit between the model containing the two parameters and the experimental data was expected for the bidisperse A5.

The optimum values of the transport parameters provide a picture of the mass transport mechanisms prevailing in the catalysts. The Knudsen flow dominated in pellets of ICI 52-1. On the other hand, the viscous flow was the most

Table 2
Optimum transport parameters and minima of the objective function (9)

Catalyst	$\sum n_j$	$\langle r\rangle\psi$ (nm)	$\langle r^2\rangle\psi$ (nm^2)	χ^2
ICI 52-1	53810	1.100	22.4	27.59
Cherox	25953	5.124	683.3	31.81
A5	14834	186.0	415700	33.74

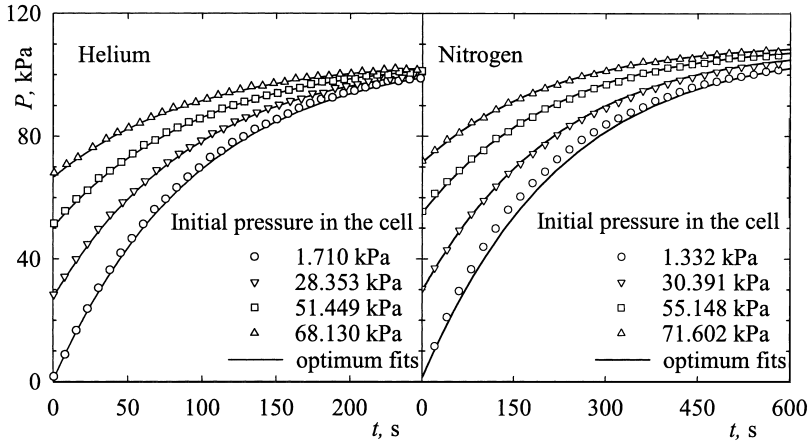

Fig. 2. Permeation of He and N_2 in Cherox. The selected responses and experimental points are only shown.

significant mechanism of mass transport in pellets of A5. To quantify it, the partial derivatives of the molar concentration of nitrogen with respect to the transport parameters of all catalysts, i.e. the sensitivity functions, are shown in Fig. 3. Generally speaking, the higher the sensitivity function value, the more sensitive the solution of initial boundary value problem is, to a small change of any parameter of interest. All the sensitivity functions are positive for any value of t, i.e. a small positive change of both the transport parameters would speed up the process of permeation. In the case of ICI 52-1 the sensitivity function $\omega_1(t)$ is much higher than $\omega_2(t)$ in the whole time domain. It is obvious the response curve, $R_gTc(t, 0)$, would be very sensitive to a small perturbation of $\langle r\rangle\psi$. On the other hand, a perturbation of $\langle r^2\rangle\psi$ would have the negligible influence on the system responses. Since pellets of Cherox and A5 have wider pores, the corresponding maxima of $\omega_2(t)$ rise. The maximum of $\omega_2(t)$ is higher than the maximum $\omega_1(t)$ for pellets of A5. In this case the system response would be most sensitive to a small perturbation of $\langle r^2\rangle\psi$.

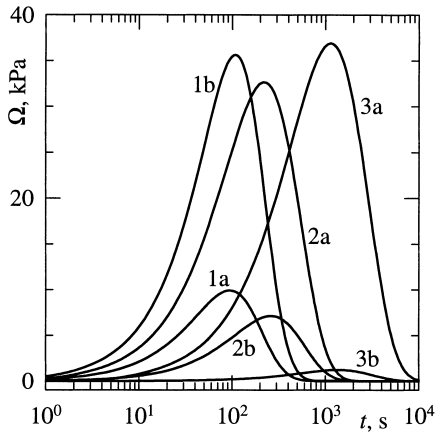

Fig. 3. Sensitivity function (10) for permeation of N_2 calculated for the optimum transport parameters. The digits designate the catalyst — 1, A5; 2, Cherox; 3, ICI 52-1. The letters 'a' and 'b' are used for $\omega_1(t)$ and $\omega_2(t)$, respectively.

The accuracy of the calculated values of the transport parameters may be judged according to their confidence limits (confidence region) [11]. The model given by Eqs. (2) and (4)–(8) is not linear in the transport parameters and, thus, the estimation of confidence limits using the variance–covariance matrix is not recommended [12]. Furthermore, it was found the variance–covariance matrix calculated from the model linearized nearby the optimum was always nondiagonal, i.e. the transport parameters were correlated significantly in all cases (correlation coefficients of the parameters $\langle r^2\rangle\psi$ and $\langle r\rangle\psi$ were -0.945 for ICI 52-1, -0.917 for Cherox, and -0.891 for A5). The correlation of these transport parameters follows from the nature of the model. In the first approximation pores can be modeled by long cylindrical capillaries in which the simple relation holds: $\langle r^2\rangle=\langle r\rangle^2$. A real pore does not have the circular cross-section and the following inequality is generally valid: $\langle r^2\rangle\neq\langle r\rangle^2$. However, it is apparent the two quantities $\langle r\rangle\psi$ and $\langle r^2\rangle\psi$ must be correlated in real pore networks. From these reasons, the correlation matrix could be used exclusively as a measure of correlation.

An alternative approach to estimation of confidence limits has been suggested by Mezaki and Kittrell [12]. According to the Beale likelihood criterion [13] it is possible to determine the critical sum of the squared deviations, χ^2_{crit}, for the 100(l−α)% confidence level and the two model parameters as follows:

$$\chi^2_{\text{crit}} = \chi^2_{\text{opt}} + 2F_\alpha(2, \nu). \tag{11}$$

where $F_\alpha(2, \nu)$ is the upper α probability point of the Fisher distribution with the two and ν degrees of freedom. In our particular case ν is defined by $\sum n_j - 2$. If the usual value of 0.0455 is assumed for α, $F_\alpha(2, \nu)$ is always 3.09. To determine the confidence limits, e.g. the upper limit of $\langle r\rangle\psi$, the task of nonlinear programming had to be solved, e.g.

$$\text{maximize } \langle r\rangle\psi \tag{12}$$

Table 3
Confidence limits of transport parameters

Catalyst	$\langle r\rangle\psi$ (nm)		$\langle r^2\rangle\psi$ (nm)		χ^2_{crit}
	Lower	Upper	Lower	Upper	
ICI 52-1	1.065	1.137	0[a]	45.2	33.77
Cherox	4.95	5.30	560	806	37.99
A5	170	202	400800	431400	39.92

[a] Approximate value.

subject to the inequality constraint

$$\langle r\rangle\psi|_{opt} < \langle r\rangle\psi < \infty \quad (13)$$

and the equality constraint given by Eq. (11).

Table 3 summarizes the confidence limits of the transport parameters $\langle r\rangle\psi$, $\langle r^2\rangle\psi$, and the critical sums of squared deviations for the 95.45% confidence level. The comparison of Tables 2 and 3 revealed that the confidence intervals were approximately symmetric and, therefore, the model was only slightly nonlinear in the transport parameters (confidence region was almost ellipse). The pellets of ICI 52-1 had narrow pores and, thus, the Knudsen flow was clearly the dominating mechanism of mass transport (see Fig. 3, $\omega_2(t)$ was negligible in comparison with $\omega_1(t)$). Under these circumstances the wide confidence interval of $\langle r^2\rangle\psi$ was not surprising. On the other hand, the first parameter $\langle r\rangle\psi$ was estimated reliably according to its narrow confidence interval. One could conclude that only the experimental conditions were suitable for the estimation of the first transport parameter. To improve the estimation of the second transport parameter, one would have to perform additional experiments under a higher mean pressure in the cell (both c^0 and P_{in} would be higher). Suitable conditions may be determined by means of sensitivity analysis. The ranges of $\omega_1(t)$ and $\omega_2(t)$ should be approximately same. The flow in pores of Cherox took place in the transition region under conditions used in this work. Fig. 3 illustrates it in terms of the sensitivity functions $\omega_1(t)$ and $\omega_2(t)$, which are not very different in their magnitudes. The confidence interval of $\langle r^2\rangle\psi$ is relatively narrowest for A5 because the viscous flow is the most significant mechanism of mass transport as one could deduce from the magnitudes of $\omega_1(t)$ and $\omega_2(t)$.

The transport parameters of Cherox found in this work were in reasonably good agreement with transport parameters of the same catalyst ($\langle r^2\rangle\psi$=895.4 nm^2, $\langle r\rangle\psi$=5.129 nm, ψ=0.267) estimated [14] from transient responses of the Wicke–Kallenbach cell.

5. Conclusions

The dynamic experimental method of transport parameter evaluation was found to be reliable for both the monodisperse and bidisperse porous media. The equipment needed for it was simple and relatively cheap. The characterization of a catalyst could be performed within 1 day. The optimum values of transport parameters were supplemented by the confidence limits. The transport parameters can be used as well for predicting the combined transport due to simultaneous pressure and composition gradients. Note that the permeation cell can be easily modified to work under different mean pressure. In this manner, the experimental conditions can be adjusted according to a porous medium texture in order to get reliable estimates of the parameters.

Acknowledgements

This work was supported by the Grant Agency of Academy of Science of the Czech Republic (Project A4072915).

References

[1] J. Valuš, P. Schneider, A novel cell for gas-counter diffusion measurements in porous pellets, Appl. Catal. 1 (1981) 355.
[2] M. Novák, K. Erhardt, K. Klusáček, P. Schneider, Dynamics of nonisobaric diffusion in porous catalysts, Chem. Eng. Sci. 43 (1988) 185.
[3] P. Čapek, V. Hejtmánek, O. Šolcová, P. Schneider, Gas transport in porous media under dynamic conditions, Catal. Today 38 (1997) 31.
[4] V. Hejtmánek, P. Čapek, O. Šolcová, P. Schneider, Dynamics of pressure build-up accompanying multicomponent gas transport in porous solids: inert gases, Chem. Eng. J. 70 (1998) 189.
[5] P. Schneider, Multicomponent isothermal diffusion and forced flow of gases in capillaries, Chem. Eng. Sci. 33 (1978) 1311.
[6] E.A. Mason, A.P. Malinauskas, Gas Transport in Porous Media: The Dusty Gas Model, Elsevier, Amsterdam, 1983.
[7] P.J.A.M. Kerkhof, A modified Maxwell–Stefan model for transport through inert membranes: the binary friction model, Chem. Eng. J. 64 (1996) 319.
[8] R.F. Sincovec, N.K. Madsen, Software for nonlinear partial differential equations, ACM Trans. Math. Software 1 (1975) 261.
[9] W.H. Press, S.A. Teukoisky, W.T. Vetterling, B.P. Flannery, Numerical Recipes in C, 2nd Edition, Cambridge University Press, Cambridge, 1992.
[10] P. Čapek, A. Seidel-Morgenstern, Sensitivity analysis of multicomponent mass transport in porous solids described by partial differential equations, in: Proceedings of the International Workshop on Scientific Computing in Chemical Engineering II, Hamburg, Germany, 26–28 May 1999.
[11] D.J. Pritchard, J. Downie, D.W. Bacon, Further consideration of heteroscedasticity in fitting kinetic models, Technometrics 19 (3) (1977) 227.
[12] R. Mezaki, J.R. Kittrell, Parametric sensitivity in fitting nonlinear kinetic models, Ind. Eng. Chem. 59 (5) (1967) 63.
[13] E.M.L. Beale, Confidence regions in nonlinear estimation, R. Statist. Soc. B 22 (1960) 41.
[14] O. Šolcová, H. Šnajdaulová, V. Heitmánek, P. Schneider, Characterization of porous solids for gas transport, in: Proceedings of the International Conference on Porous Structure — COPS V, Heidelberg, Germany, 30 May–2 June 1999, in press.